Mon. Not. R. Astron. Soc. **346,** 1215–1230 (2003)

The star formation rate in disc galaxies: thresholds and dependence on gas amount

S. Boissier,[1⋆] N. Prantzos,[2] A. Boselli[3] and G. Gavazzi[4]

[1] *Carnegie Observatories, 813 Santa Barbara Street, Pasadena, CA 91101, USA*
[2] *Institut d'Astrophysique de Paris, 98bis Bd Arago, 75104 Paris, France*
[3] *Laboratoire d'Astrophysique de Marseille, Traverse du Siphon, F-13376 Marseille Cedex 12, France*
[4] *Universita degli Studi di Milano, Bicocca, Pizza dell'Ateneo Nuovo 1, 20126 Milano, Italy*

Accepted 2003 September 3. Received 2003 September 2; in original form 2003 July 22

ABSTRACT

We reassess the applicability of the Toomre criterion in galactic discs and we study the local star formation law in 16 disc galaxies for which abundance gradients are published. The data we use consist of stellar light profiles, atomic and molecular gas (deduced from CO with a metallicity-dependent conversion factor), star formation rates (from Hα emissivities), metallicities, dispersion velocities and rotation curves. We show that the Toomre criterion applies successfully to the case of the Milky Way disc, but it has limited success with the data of our sample; depending on whether or not the stellar component is included in the stability analysis, we find average values for the threshold ratio of the gas surface density to the critical surface density in the range 0.5–0.7. We also test various star formation laws proposed in the literature, i.e. either the simple Schmidt law or modifications of it, that take into account dynamical factors. We find only small differences among them as far as the overall fit to our data is concerned; in particular, we find that all three star formation laws (with parameters derived from the fits to our data) match observations in the Milky Way disc particularly well. In all cases we find that the exponent n of our best-fitting star formation rate has slightly higher values than in other recent works and we suggest several reasons that may cause that discrepancy.

Key words: galaxies: evolution – galaxies: general – galaxies: spiral.

1 INTRODUCTION

Star formation is the main driver of galactic evolution. Despite four decades of intense observational and theoretical investigation (see, e.g., Elmegreen 2002 for a recent overview) our understanding of the subject remains frustratingly poor. As a result, important questions related, for example, to the putative threshold and to the rate of star formation in galaxies have no clear answers yet.

In most (if not all) studies of galaxy evolution, empirical formulae are used to describe the star formation. Such formulae are based on the original suggestion by Schmidt (1959), namely that the star formation rate (SFR) is simply proportional to some power n of the gas mass density ρ. In the case of disc galaxies and starbursts observations (Kennicutt 1998b) suggest that such a relation indeed holds when the gas surface density $\Sigma_{\rm gas}$ is used instead of the mass density and when quantities are averaged over the whole optical disc; in that case, the exponent n is found to be close to 1.5. However, Kennicutt (1998b) noted that other interpretations of the data are possible: in particular, an equally good fit to the data is obtained when it is assumed that gas turns into stars within a dynamical time-scale (taken to be the orbital time-scale at the optical radius).

Such 'global' laws may be useful for some applications (such as, for example, semi-analytical models of galaxy evolution) but for detailed models of galactic discs 'local' star formation (SF) laws are required. Several such laws have been suggested either on observational (e.g. Dopita & Ryder 1994) or theoretical grounds (e.g. dynamical instabilities in spirals, Ohnisi 1975; Wyse & Silk 1989). In a recent work, Wong & Blitz (2002) find that the simple Schmidt law is valid locally, with $n = 1.1$–1.7 (depending on whether extinction on the observed Hα emissivity profiles of their discs is assumed to be uniform or dependent on gas column density). They also find that a dynamically modified Schmidt law (i.e. by introducing the orbital time-scale as Kennicutt 1998b) also gives an acceptable fit to their data.

The question of a threshold in star formation in galactic discs has been assessed observationally by Kennicutt (1998b), who found that star formation is strongly suppressed below $\Sigma_{\rm gas} \sim 5$–$10\ {\rm M}_{\odot}\ {\rm pc}^{-2}$. The existence of such a threshold is indeed suggested by dynamical stability analysis of thin, gaseous, differentially rotating discs (e.g. Toomre 1964; Quirk 1972). In a recent investigation, Martin & Kennicutt (2001) found that the threshold gas density (measured at the edge of the star-forming disc) varies by at least an order of

⋆E-mail: boissier@ociw.edu

magnitude among spiral galaxies, but the ratio of gas density to a critical density (see Section 4 for its definition) is much more uniform. Martin & Kennicutt (2001) also identified the limitations of their observational strategy: uncertainties associated with non-axisymmetric gas distributions and with the extrapolation of the molecular gas density profile, from the last observed point to the edge of the star-forming disc. The latter issue was properly studied by Wong & Blitz (2002) with the help of detailed molecular profiles, but for a limited sample of spirals, particularly rich in molecular gas. Their conclusion is that the gravitational stability criterion has only a limited application.

From the theoretical point of view, quite a lot of work has been performed to include more physics in the analysis than the simple stability criterion (e.g. Toomre 1981; Elmegreen 1987; Romeo 1992; Wang & Silk 1994, etc.) The general conclusion is that the various physical factors (stars, magnetic fields, turbulence) affect the stability parameter only slightly, by a factor of the order of unity.

In a recent work Schaye (2002) reassesses the role of the gas velocity dispersion in the application of the simple stability criterion. He suggests that the usual assumption of a constant dispersion over the disc may not hold and he investigates the stability of thin, gaseous, self-gravitating discs embedded in dark haloes and illuminated by UV radiation. He finds that the drop in the velocity dispersion associated with the transition from a warm to a cold phase of the interstellar medium (i.e. from $\sim 10^4$ K to below 10^3 K) causes the disc to become gravitationally unstable. This analysis leads to prescriptions for evaluating threshold surface densities as a function of metallicity, intensity of UV radiation, and gaseous fraction. However, a major prediction of his model analysis seems to be contradicted by observations. Indeed, he finds that at the phase transition there is always a sharp increase in the molecular gas fraction, whereas Martin & Kennicutt (2001) find that at the thresholds of their star-forming discs the gas is primarily atomic (for the low gas surface densities) or molecular (for the highest gas surface densities), i.e. no clear sign of a phase transition.

In this work, we reassess the applicability of the Toomre criterion in galactic discs and we study the local star formation law by means of a homogeneous sample containing 16 spirals, half of which belong to the Virgo cluster. In Section 2 we present our data sample, which consists of profiles of stars, atomic and molecular gas, star formation rates (from Hα emissivities), metallicities and rotation curves. In Section 3 we present briefly the theoretical background of the stability criterion, including a modification suggested by Wang & Silk (1994). We show that it applies successfully to the case of the Milky Way disc (Section 3.2) but it has limited success with the data of our sample. In Section 4 we test various SF laws proposed in the literature, i.e. either the simple Schmidt law or modifications of it, that take into account dynamical factors. We find only small differences among them as far as the overall fit to our data is concerned; in particular, we find that all three SF laws (with parameters derived from the fits to our data) match particularly well observations in the Milky Way disc. In all cases we find that the exponent n of our best-fitting SFR has slightly higher values than in other recent works and we suggest several reasons that may cause that discrepancy. Our results are summarized in Section 5.

2 OBSERVATIONAL DATA

2.1 The galaxy sample

The galaxies of our sample were selected for a detailed study of the star formation properties in nearby spirals. Our first requirement was that abundance measurements in H II regions are available so that a metallicity gradient is defined. The molecular gas profile can then be deduced from CO observations with a metallicity-dependent conversion factor recently determined (see Boselli, Lequeux & Gavazzi 2002 and Section 2.3 below). For this reason, these galaxies do not form a complete sample in any sense but are those for which the metallicity-dependent conversion factor can be used. An accurate estimate of the radial profile of atomic gas and of the star formation rate (here deduced from Hα emission-line intensities) is also required for our purpose. Some of the proposed instability criteria in galactic discs involve the rotation frequency (requiring knowledge of the rotation curve), the stellar surface density profile (obtained from the H- and K-band profiles), and also the velocity dispersion of the stellar component (derived in Section 3.1).

The final list of galaxies, only selected to have abundance gradients published and the other data needed for our analysis, includes 16 galaxies, seven of them 'isolated' and nine belonging to the Virgo cluster (most of the data concerning the Virgo galaxies are available via the goldmine data base, Gavazzi et al. 2003). Note that some of the 'isolated' galaxies are in fact part of small groups (NGC 2403, 3031, 4258, 5194).

In order to estimate the degree of perturbation induced by the interaction of a galaxy with its environment, we use the H I *deficiency parameter*, defined as H I def. $= \log(\langle \mathrm{H\,I} \rangle / \mathrm{H\,I})$, the ratio of the average H I mass in isolated objects of similar morphological type and linear size to the H I amount of an individual galaxy (Haynes & Giovanelli 1984). The sample includes both gas deficient (H I def. $>$ 0.3) and gas-rich galaxies to study whether their SFR profiles are affected by the amount of gas available. It has been selected to span the largest possible range in gas column density within late-type galaxies of similar type.

Information on the galaxies of the adopted sample is given in Table 1. Column 1 gives the name of the galaxy and column 2 the blue magnitude. Column 3 gives the galaxy distance. A distance of 17 Mpc is adopted for all the Virgo galaxies. We adopt the distance deduced from the brightest stars of NGC 2903 (Drozdovsky & Karachentsev 2000) and the planetary nebulae distance of NGC 5194 by Feldmeier, Ciardullo & Jacoby (1997). For the other galaxies of the sample, Cepheid distances were deduced within the framework of the *HST* key project (Freedman et al. 2001). Column 4 gives the morphological type. Column 5 gives the logarithm of the H I velocity width W_C (in km s^{-1}), corrected for inclination as in Gavazzi (1987). Column 6 gives the H I deficiency, computed as in Haynes & Giovanelli (1984), from the integrated H I masses (Huchtmeier & Richter 1989) and the blue major axes as given in the Uppsala General Catalogue (Nilson 1973).

For each of our galaxies, Table 1 also provides references for the adopted profiles of neutral gas, CO emissivity and oxygen abundance data (columns 7–9, respectively). Column 10 presents the sources of the Hα data. For the majority of the sample we adopt the results of Boselli & Gavazzi (2002); for three galaxies (m) we use the data kindly made available by Martin & Kennicutt (2001) and for three others (n) data obtained by Hippelein et al. (in preparation).

Column 11 gives references for rotation curves. Finally, column 12 gives the photometric bands for which we have images, allowing to derive corresponding stellar surface density profiles.

For NGC 3031 and 4258, we used the H-band profile provided in the 2MASS large galaxies atlas: http://www.ipac.caltech.edu/2mass/gallery/largegal/ (Jarrett et al. 2002).

Table 1. The sample of galaxies used in this study. Properties are given in columns 2–6 and references for the data in columns 7–11. The description of the table entries is given in Section 2. The first half of the table concerns nearby galaxies, while the second half refers to Virgo galaxies.

Galaxy (1)	m_B (mag) (2)	Dist. (Mpc) (3)	Type (4)	log(W_C) (5)	H I def. (6)	H I (7)	CO (8)	Z (9)	H_α (10)	$V(R)$ (11)	Photometry (12)
NGC 925	10.69	9.16	SAB(s)d	2.42	0.0	a	f	i, j	o	p	*B*, *V*, *H*
NGC 2403	8.93	3.22	SAB(s)cd	2.47	0.1	a	h	i,j, k	o	q, r	*B*, *V*, *H*, *K*
NGC 2541	12.26	11.22	SA(s)cd	2.33	0.7	b	g	j	o	s	*U*, *B*, *V*, *H*
NGC 2903	9.68	8.90	SB(s)d	2.65	0.4	a	h	i, j	o	q, r	*U*, *B*, *V*, *H*
NGC 3031	7.89	3.63	SA(s)ab	2.67	0.1	c	f	j	o	r, t	*B*, *V*, *H*
NGC 4258	9.10	7.98	SAB(s)bc	2.68	0.5	a	h	j	o	r, u	*B*, *V*, *H*
NGC 5194	8.96	8.40	SA(s)bc-pe	2.76	0.6	d	h	j	o	r	*B*, *V*, *H*
NGC 4254	10.44	17.00	SA(s)c	2.76	0.0	e	h	l	o	v, w, x	*B*, *V*, *H*
NGC 4303	10.18	17.00	SAB(rs)bc	2.47	−0.1	e	h	l	n	r, x, y, z	*B*, *V*, *H*
NGC 4321	10.05	17.00	SAB(s)bc	2.73	0.5	e	h	l	o	r, x, y	*U*, *B*, *V*, *H*
NGC 4501	10.36	17.00	SA(rs)b	2.79	0.5	e	h	l	o	x, y, z	*U*, *B*, *V*, *H*
NGC 4571	11.82	17.00	SA(r)d	2.66	0.5	e	h	l	m	y	*B*, *H*
NGC 4651	11.39	17.00	SA(rs)c	2.72	−0.2	e	h	l	m	y, z	*H*
NGC 4654	11.10	17.00	SAB(rs)cd	2.56	−0.3	e	h	l	n	v, x, y	*B*, *V*, *H*, *K*
NGC 4689	11.60	17.00	SA(rs)bc	2.47	0.9	e	h	l	n	v, x, y	*B*, *V*, *K*
NGC 4713	12.19	17.00	SAB(rs)d	2.35	−0.4	e	–	l	m	v, y	*V*, *H*

References: Wevers et al. (1986) [a], Broeils & van Woerden (1994) [b], Rots (1975) [c], Rand et al. (1992) [d], Warmels (1986) [e], Sage (1993) [f], Braine et al. (1993) [g], Young et al. (1995) [h], van Zee et al. (1998) [i], Zaritsky et al. (1994) [j], Garnett et al. (1997) [k], Skillman et al. (1996) [l] Martin & Kennicutt (2001) [m], Hippelein et al., in preparation [n], Boselli & Gavazzi (2002) [o], Pisano et al. (1998) [p], Begeman (1987) [q], Sofue et al. (1999) [r], Vega Beltrán et al. (2001) [s], Adler & Westpfahl (1996)[t], van der Kruit (1974) [u], Sperandio et al. (1995) [v], Chincarini & de Souza (1985) [w]. Guhathakurta et al. (1988) [x], Rubin et al. (1999) [y], Distefano et al. (1990) [z]. The images from which the photometric data are derived are presented for the Virgo galaxies in Boselli et al. (1997, 2000) (H) and Boselli, Gavazzi & Sanvito 2003 (optical). For the other galaxies in the infrared: Pierini et al. (1997), Boselli et al. (2000), Zibetti et al., in preparation. The optical data will be presented in a subsequent paper making greater use of them (Boissier et al., in preparation).

2.2 Atomic gas profiles

With the exception of NGC 5194 (H I map obtained with the VLA), the data were obtained with the Westerbork Radio Telescope (see the caption of Table 1). The H I profile given by Broeils & van Woerden (1994) was obtained along the major axis of the galaxy. The data by Wevers, van der Kruit & Allen (1986), Rots (1975) and Rand, Kulkarni & Rice (1992) were obtained by integrating H I maps over concentric ellipses.

The data concerning the Virgo galaxies are taken from the thesis of Warmels (1986). His data are two-dimensional maps for NGC 4321, 4501 and 4651. For the other galaxies, the data were obtained along one (and sometimes two) resolution axis. The maps were integrated on to one resolution axis, and the same procedure was applied to the whole sample to obtain the H I density profiles from the data along one axis.

In all the cases, the H I profiles correspond to a 'face-on' orientation. A typical uncertainty of 20 per cent should be quoted for all the H I profiles, which is smaller than the uncertainties of H_2 profiles (see the next section).

2.3 Molecular gas profiles

The adopted CO intensity profiles have been corrected for inclination. The spatial resolution of the CO observations is relatively poor (45arcsec) and the measurements were made only along the major axis of each galaxy. On the other hand, the relatively large beams average the CO emission on larger scales and are less affected by small-scale clumpiness.

In their recent study concerning the star formation rate in galactic discs, Wong & Blitz (2002) used high-resolution profiles obtained with the BIMA interferometer (Regan et al. 2001) for seven disc galaxies. The observations of Regan et al. (2001) concern 15 galaxies from which four are in common with our sample (NGC 2903, 4258, 5194, 4321). Their profiles (fig. 3 in Regan et al. 2001) differ from ours in the innermost parts of the galaxies, but we are only interested in galactic discs and not in bulges in this work, so that this difference is not of importance for our conclusions.

The low-resolution CO profiles adopted in this work are obviously missing any small-scale structure seen in the high-resolution profiles of Regan et al. (2001). Our profiles, however, agree well with the low-resolution one also shown in Regan et al. (2001, fig. 3), which represent a good estimate of the average CO profile in most cases. Among the four galaxies that are common in the two samples, only NGC 4258 presents really important variations (∼1 mag) on small scales.

The uncertainty on the H_2 content is much larger than that of the CO data; it is also more difficult to quantify, since it depends on the poorly known factor X converting CO to H_2. In a recent work Boselli et al. (2002), based on spectro-photometric data available for a small number of nearby galaxies and on a larger sample of late-type galaxies with multifrequency data, found that X depends on metallicity (or luminosity) and they parametrized that dependence as

$$\log X = -1.01[12. + \log(\mathrm{O/H})] + 29.28, \quad (1)$$

i.e. the conversion factor is essentially inversely proportional to metallicity. While this correlation was found for integrated values over whole galaxies, we make the assumption that it is also valid for radial profiles. This assumption agrees with the analysis of M51 performed by Nakai & Kuno (1995) that, based on the measured radial variation of the dust-to-gas ratio, brought to similar results.

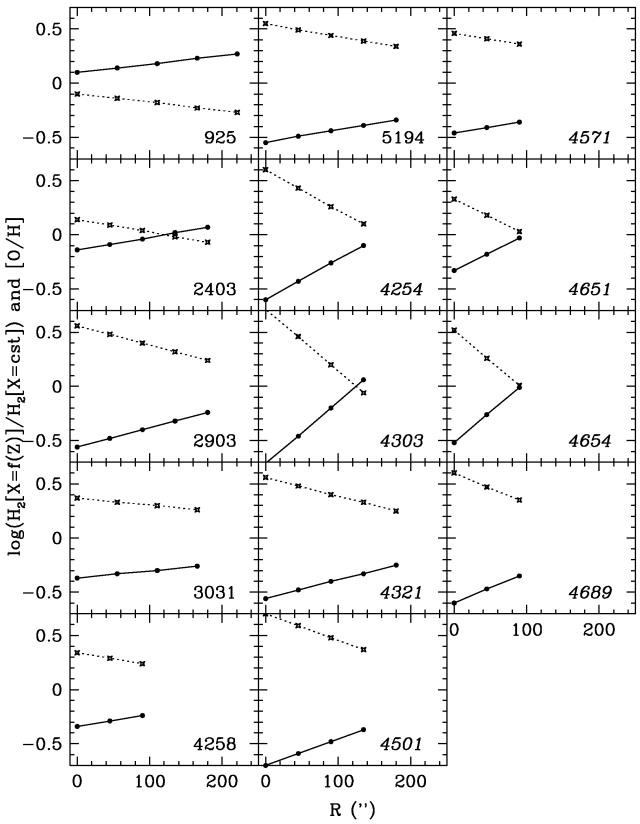

Figure 1. Solid curves, amount of molecular gas obtained by our method (i.e. with the metallicity-dependent conversion factor of CO to H_2), divided by the amount of molecular gas obtained with a constant conversion factor. Results are plotted as a function of galactocentric radius. Dotted curves, the corresponding metallicity profiles $[O/H] = \log(O/H) - \log(O/H)_\odot$. As in the following figures, the name of the Virgo galaxies is indicated in italic.

We transformed CO data into molecular H_2 surface density using the metallicity-dependent conversion factor of equation (1). We note that the resulting H_2 profile is much poorer in molecular gas, especially in inner galactic regions, than profiles obtained with a constant factor. In Fig. 1 we show the ratio of the two profiles i.e. that obtained with a metallicity-dependent X divided by that obtained with a constant X. It is clearly seen that differences by a factor of 2–3 in the inner galaxy are usually obtained.

We note that Wong & Blitz (2002) use a constant conversion factor X, as in fact do most studies of SFR in the literature. This explains part of the differences between our study and others (see the discussion in Section 4.2).

2.4 Star formation rate profiles

The star formation rate profiles were obtained by subtracting the radial profiles of the continuum near Hα from the Hα + [N II] radial profiles. For three of our galaxies, we used Hα profiles of Martin & Kennicutt (2001), kindly provided by the authors.

The Hα flux was integrated along elliptical annuli with the same PA and inclination as for the H I (see Table 2 for the adopted values). It was corrected for inclination, and translated to a star formation rate as in Boselli et al. (2001). Hα + [N II] fluxes were corrected for [N II] contamination and internal extinction (see Boselli et al. 2001). The conversion from *extinction-corrected* Hα flux to star formation rate is obtained assuming a power-law IMF of slope −2.5 between 0.1 and 80 $M_\odot$:

$$\mathrm{SFR}\ (M_\odot\ \mathrm{yr}^{-1}) = 0.8610^{-41} L_{H\alpha}\ (\mathrm{erg\ s}^{-1}).$$

As estimated in Boselli et al. (2001), the uncertainties in the IMF, extinction and [N II] contamination correction result in an overall uncertainty of the absolute SFR of a factor of ∼3.

We note that Wong & Blitz (2002) applied radially dependent extinction corrections to Hα, using the observed gas profiles, an assumed dust-to-gas ratio, and a given geometry between H I, H_2 and the stars. We prefer here to apply a simple correction for the whole galaxy since, as stressed in Martin & Kennicutt (2001), 'radial gradients in internal extinction are typically not strong compared with the scatter in extinction at a given radius'. Moreover, the approach of Wong & Blitz (2002) does not take into account the existence of an abundance gradient within the discs, which is likely to affect the dust-to-gas ratio in different ways at different radii.

Table 2. Parameters adopted for the determination of the Hα and photometric profiles.

Galaxy	Inclination (deg)	PA (deg)
NGC 925	54.00	102
NGC 2403	60.00	125
NGC 2541	66.80	−29
NGC 2903	60.00	29
NGC 3031	68.00	332
NGC 4258	63.00	330
NGC 5194	20.00	163
NGC 4254	24.51	56
NGC 4303	35.99	7
NGC 4321	27.37	153
NGC 4501	58.62	140
NGC 4571	21.09	55
NGC 4651	45.24	71
NGC 4654	59.05	128
NGC 4689	41.01	55
NGC 4713	47.80	100

2.5 Metallicity profiles

In order to compute the conversion factor X from CO to H_2, we need the metallicity as a function of radius. Zaritsky, Kennicutt & Huchra (1994), van Zee et al. (1998), Garnett et al. (1997) and Skillman et al. (1996) measured with the same method the oxygen abundances in H II regions located at various galactocentric radii in the sample of our galaxies. From their data, they derived an abundance gradient (slope and intersect at the centre of the galaxy) that we use to estimate the metallicity at each radius (see Fig. 1).

2.6 Photometry

The photometric profiles obtained within the framework of our project were treated in a similar way to the Hα profiles (i.e. they were integrated over ellipses with the same position angle and inclination, given in Table 2). In Fig. 2, we present the B- and H-band profiles, which are the most useful for the present work.

We derive a scalelength h_B by an exponential fit to the disc part of the B-band profiles (to be used in Section 3.1). The H-band profiles, unaffected by dust extinction, have been used in order to estimate the stellar mass density, assuming the same mass-to-light ratio as in

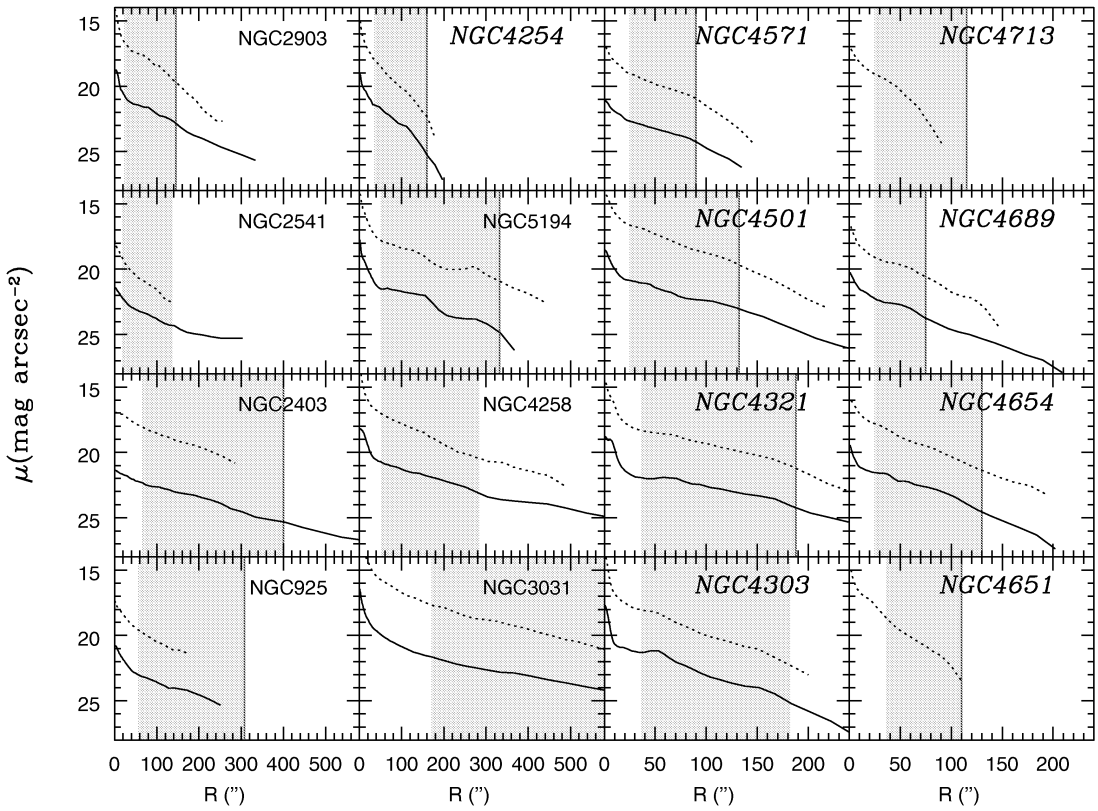

Figure 2. Surface brightness radial profiles in the *B* band (solid curves) and in the *H* band (dotted curves) for the galaxies of our sample. The grey area is the 'disc' region, used for the study of the SFR properties. Its outer radius is either the Martin & Kennicutt (2001) 'cut-off' (vertical line, as in Fig. 5) or our own 'cut-off' (Section 2.8). Its inner radius is the point where the bulge starts dominating over the disc (Section 2.6). This figure is available in colour in the on-line version of the journal on *Synergy*.

Boissier et al. (2001). In the case of NGC 4689 the stellar profile was scaled from the *K*-band profile (since the *H*-band profile was not available), taking into account the total magnitudes in *H* and *K* bands, respectively, $H = 8.32$ and $K = 7.76$ (Boselli et al. 1997).

An inspection of the profiles (Fig. 2) shows that in the inner 1 or 2 kpc they present departures from the exponential disc profile, obviously due to the presence of a bulge. These inner regions are ignored in our analysis.

2.7 Rotation curves

The rotation curves of the galaxies of our sample are obtained through a variety of sources: H I rotation curves of Pisano, Wilcots & Elmegreen (1998), Begeman (1987), Adler & Westpfahl (1996) and Guhathakurta et al. (1988), rotation curves derived from optical spectroscopy by van der Kruit (1974), Vega Beltrán et al. (2001), Chincarini & de Souza (1985), Distefano et al. (1990) and for the Virgo galaxies by Rubin, Waterman & Kenney (1999) and Sperandio et al. (1995). For seven of our galaxies, high-resolution curves are given by Sofue et al. (1999), resulting from a combination of CO, optical and H I data.

The adopted rotation curves are presented in Figs 3 and 4 for isolated and Virgo galaxies, respectively. In those figures we also indicate by a horizontal line half the value of W_C (the H I linewidth), in order to show the difference with respect to a flat rotation curve. This constant value usually represents well the 'plateau' of the rotation curves, which is not reached at the same radius for all the galaxies. It should be noted that the data originate from different sources (i.e. studies with different angular resolutions) and present a substantial amount of scatter. For the purpose of homogeneity we approximated the rotation curves with the simple function:

$$V(R) = 0.5 W_C [1 - \exp^{(-R/R_V)}]. \quad (2)$$

At large radii, this approximation produces a plateau at the value W_C given by the H I linewidth. At small radii, the parameter R_V controls the rise of curve. R_V was adjusted for each galaxy, allowing the curve of equation (2) to reproduce satisfactorily the observed one. This simple representation has the advantages that: (i) it provides a uniform description of the rotation curve for all galaxies; (ii) it has only one free parameter; and (iii) it can be derived analytically, a useful property for the study of stability criteria in discs (see Section 3).

2.8 Comments

Our H_2, H I and SFR surface density profiles are displayed in Fig. 5. Several points should be noted concerning these profiles.

(i) Resolution is quite different in the profiles of the three major quantities studied. It is low in the case of H_2, where only three to five points are available along the disc; it is satisfactory in the case of H I, with more than 20 points per galaxy, on average; and it is excellent in the case of the Hα profile, where a large number of features appear on the corresponding curves, resulting from azimuthally averaging across the spiral arms. Even if we made an enormous effort of homogenization, the data are not as deep at all wavelengths, in particular for H_2.

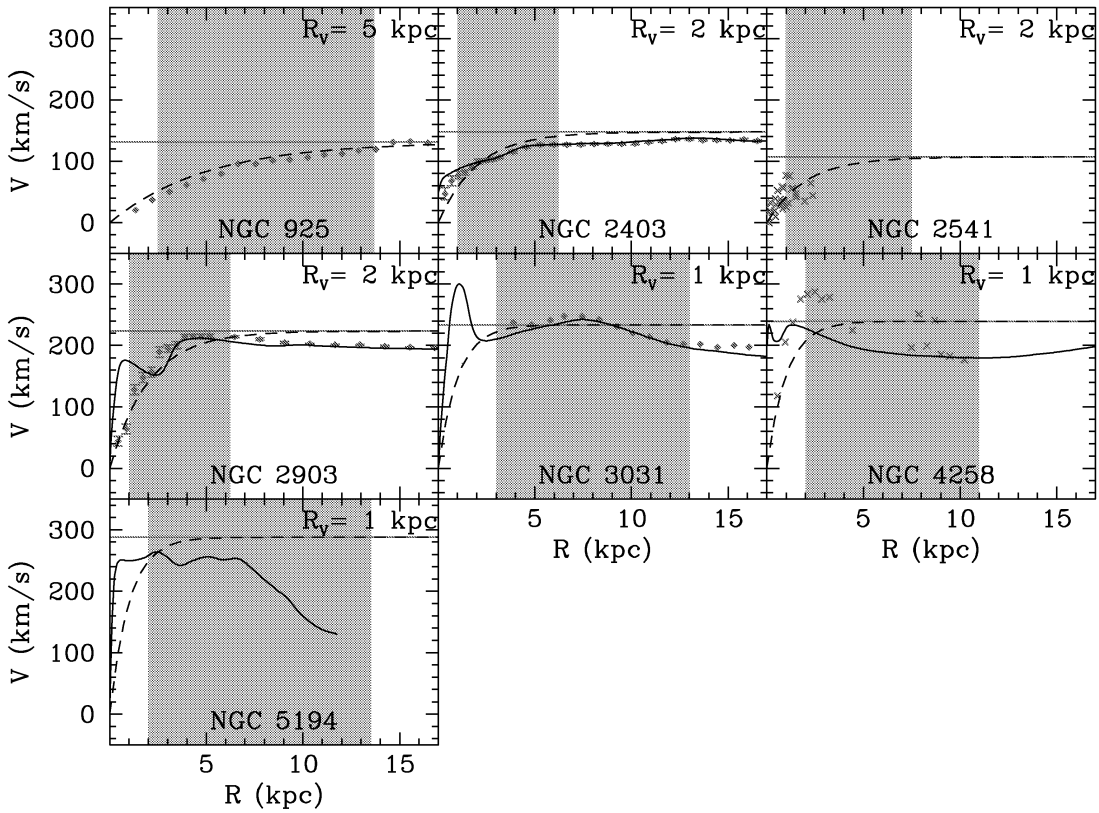

Figure 3. Rotation curves for the isolated galaxies of our sample. Diamonds, H I data (Pisano et al. 1998 for NGC 925, Begeman 1987 for NGC 2403 and 2903, Adler & Westpfahl 1996 for NGC 3031). Crosses, optical slit spectra (van der Kruit 1974 for NGC 4258, Vega Beltrán et al. 2001 for NGC 2541). The solid curve indicates the composite rotation curve of Sofue et al. (1999). The horizontal line indicates half the value of the H I linewidth. The dashed curve is the function of equation (2), with the corresponding value of R_V indicated for each galaxy. Shaded areas indicate the disc region, used for the study of the star formation.

(ii) In most cases, the molecular gas dominates the inner disc, with the exception of NGC 2403, 4654 and 925 (three H I deficient discs). However, its surface density rarely exceeds 10 $M_\odot$ pc^{-2}. Only in one case (NGC 5194) does it become as large as 40 $M_\odot$ pc^{-2}.

(iii) In general, the H I disc is more extended than the SFR profile and the latter is more extended than the H_2 profile. In more than half of the cases the SFR becomes negligible (or declines strongly) at the outer limit of the molecular disc. The accurate determination of the molecular gas profile, however, is strongly limited by the difficulty of detecting CO in the low-metallicity, cold outer disc. We shall return to this point concerning a 'cut-off' of the SFR in the next section.

3 STABILITY CRITERIA AND SFR THRESHOLD

3.1 Theoretical background

The data presented in Figs 2–5 allow the question of a threshold of the SFR in disc galaxies to be assessed. Such a threshold has been suggested on both observational and theoretical grounds. On the observational side, support comes from the fact that the gaseous layer (H I) is often observed to extend much beyond the stellar disc. On the other hand, the formulation of local instability criteria for differentially rotating discs (Toomre 1964) leads naturally to the idea that large-scale star formation may occur only above a critical gas surface density. According to Quirk (1972) this happens when the Toomre parameter

$$Q = \frac{\Sigma_{\rm crit}}{\Sigma_{\rm gas}} < 1, \tag{3}$$

where $\Sigma_{\rm gas}$ is the gas surface density and $\Sigma_{\rm crit}$ is given by

$$\Sigma_{\rm crit} = \frac{\kappa \sigma_{\rm gas}}{\pi G}, \tag{4}$$

where $\sigma_{\rm gas}$ is the local gas velocity dispersion and κ is the local epicyclic frequency, given by

$$\kappa^2 = \frac{2V_{\rm C}}{R}\left(\frac{{\rm d}V_{\rm C}}{{\rm d}R} + \frac{V_{\rm C}}{R}\right), \tag{5}$$

where $V_{\rm C}$ is the gas circular velocity of the galaxy at radius R. For flat rotation curves one has $\kappa = \sqrt{2}V_{\rm C}/R = \sqrt{2}\Omega$, where Ω is the rotational frequency of the disc.

The gas velocity dispersion in the radial direction is of the order of 5–10 km s^{-1}, as derived by observations of, for example, Sanders, Solomon & Scoville (1984) in the Milky Way. In external galaxies, gas velocity dispersions obtained by Dickey, Hanson & Helou (1990) and Boulanger & Viallefond (1992) span a similar range of values and they present rather flat profiles, i.e. independent of radius (except in the inner parts of the discs where they increase, but by a factor never exceeding ~2). On theoretical grounds the gas velocity dispersion is expected to vary little in self-regulated discs (Silk 1997). In that case, one obtains for discs with flat rotation curves $\Sigma_{\rm crit} \propto \kappa \propto R^{-1}$. Since this gradient of $\Sigma_{\rm crit}$ is shallower than the observed decline of the gas surface density, it is expected

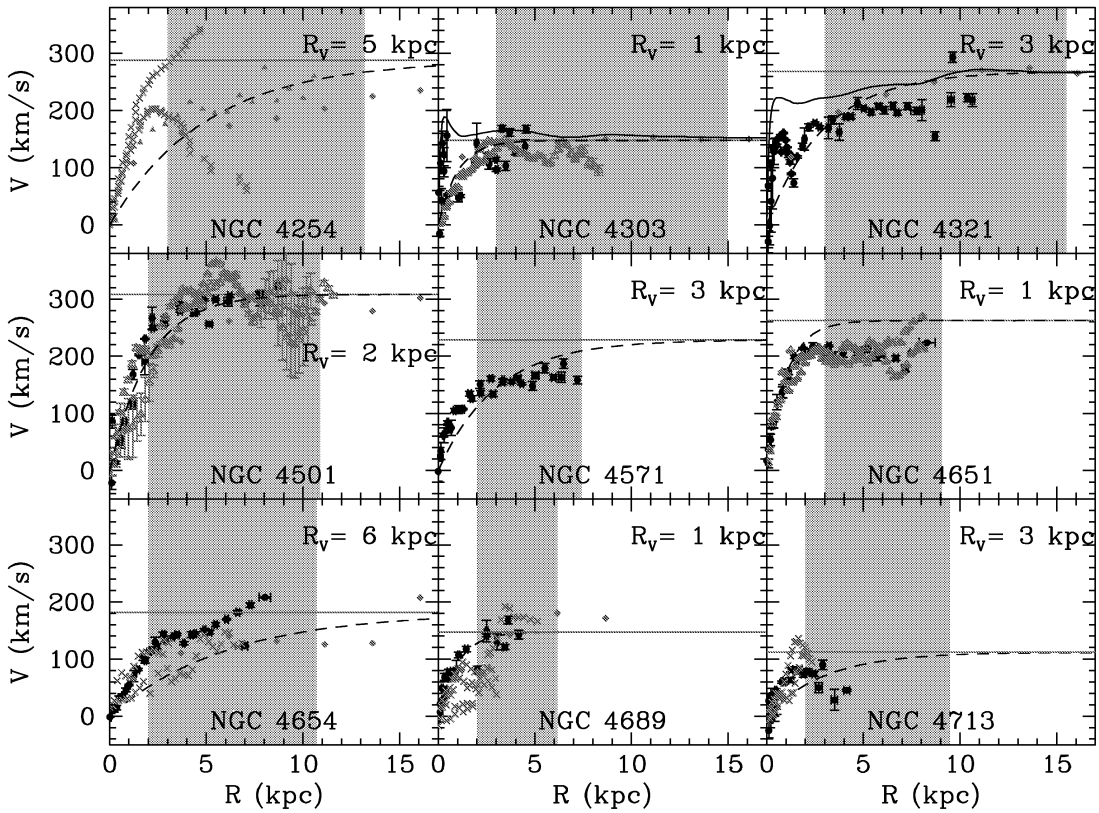

Figure 4. Rotation curves for the Virgo galaxies of our sample. Diamonds, H I data (Guhathakurta et al. 1988). Data of optical slit spectra are from Rubin et al. (1999) (filled circles) and Sperandio et al. (1995) (open circles). The solid curve indicates the composite rotation curve of Sofue et al. (1999). As in Fig. 3, the horizontal line indicates half the value of the H I linewidth, the dashed curve is the function of equation (2), with the corresponding value of R_V indicated for each galaxy, shaded areas indicate the disc region, used for the study of the star formation.

that $Q > 1$ at some 'cut-off' radius, resulting naturally in a threshold of the SFR.

These ideas were studied in a seminal paper by Kennicutt (1989), with a sample of 15 (mostly late-type) spirals. Using a constant gas velocity dispersion $\sigma_{\rm gas} = 6$ km s^{-1} he found that star formation declines rapidly in disc regions with $Q > 1.6$, i.e. for $\Sigma_{\rm gas} < 0.6\Sigma_{\rm crit}$. He also found that Q varies little within the star-forming disc, an indication of self-regulating star formation.

Wang & Silk (1994) proposed to take into account the stellar contribution to the instability by rewriting the critical density as

$$\Sigma_{\rm crit} = \gamma \frac{\kappa \sigma_{\rm gas}}{\pi G}, \quad \text{with} \quad \gamma = \left(1 + \frac{\Sigma_* \sigma_{\rm gas}}{\Sigma_{\rm gas} \sigma_*}\right)^{-1}, \tag{6}$$

where Σ_* and σ_* are, respectively, the stellar surface density and the *radial* stellar velocity dispersion.

In the rest of Section 3 we study the instability criterion of equation (3) for galactic discs using both definitions (4) and (6) for $\Sigma_{\rm crit}$. In the former case, we adopt a constant value $\sigma_{\rm gas} = 6$ km s^{-1} for the gas velocity dispersion. In the latter, a knowledge of the radial stellar velocity dispersion is also required.

As shown by Bottema (1993), the radial stellar velocity dispersion of a disc is exponentially decreasing with the galactocentric radius; the corresponding scalelength is equal to twice that observed in the B band:

$$\sigma_*(R) = \sigma_0 \exp(-R/2h_B). \tag{7}$$

Moreover, Bottema (1993) showed that the value of the radial stellar velocity dispersion at one scalelength is comparable to the vertical stellar velocity dispersion at the centre of the galaxy. He also showed that the stellar velocity dispersion in a galactic disc is correlated with its rotational velocity $V_{\rm C}$ (Fig. 6). We computed a simple fit to his data (for the more reliable inclined galaxies) to obtain

$$\sigma_*(R = h_B)\ [\text{km s}^{-1}] = -4.3 + 0.3Vc\ [\text{km s}^{-1}], \tag{8}$$

i.e. the velocity dispersion of the stellar component is ∼one-third of the rotational velocity of the disc. In the same figure we display the recent data obtained by Vega Beltrán et al. (2001) concerning the kinematics of 20 disc galaxies. Despite some scatter, these data confirm the trend found by Bottema (1993). For eight galaxies of our sample, central dispersion velocities are given by McElroy (1995). Assuming the same radial dependence as in equation (7), we computed the corresponding dispersion at one scalelength and also plotted it in Fig. 6; the results for the discs of our sample are clearly in agreement with the aforementioned trend. In the following we use these stellar velocity dispersions to calculate the value of $\Sigma_{\rm crit}$, according to equation (6).

3.2 Application to the Milky Way

Before studying the above stability criteria with our sample of disc galaxies, we present in Fig. 7 an application to the Milky Way disc. In the upper panel we show the observed profiles of the total gas surface density (H_2+H I, increased by 40 per cent to include He contribution), the stellar profile (exponential, with a scalelength of 2.5 kpc and normalized to 42 $M_\odot$ pc^{-2} in the solar neighbourhood), and the profile of the stellar radial velocity dispersion, calculated according

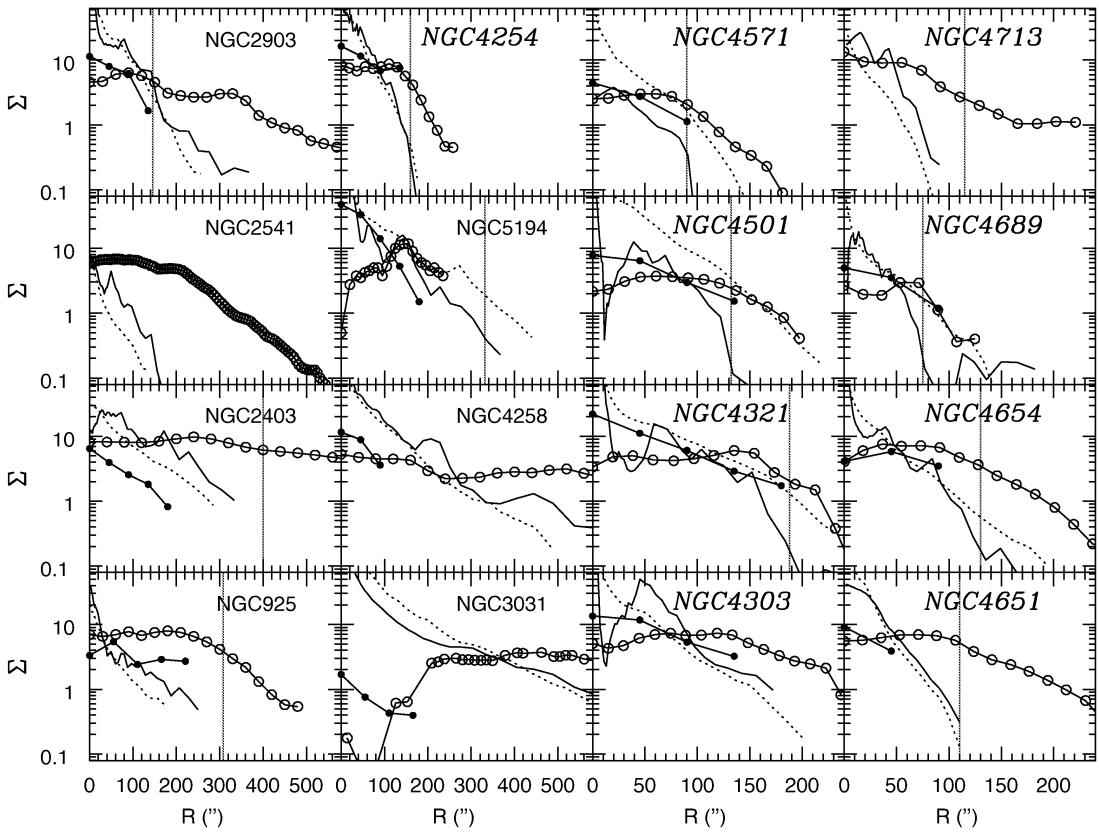

Figure 5. Surface density radial profiles of H I (open circles), H_2 (filled circles), star formation rate (solid curves), and Stellar density (dotted curves). The surface densities of H I and H_2 are in $M_\odot$ pc^{-2}, of stars in 10 $M_\odot$ pc^{-2} and of the star formation rate in $M_\odot$ pc^{-2} Gyr^{-1}. The vertical line in some of the panels indicates the SFR 'cut-off' found by Martin & Kennicutt (2001). In most cases that line coincides with (or is very close to) a region of steep decline in our own SFR profile. This figure is available in colour in the on-line version of the journal on *Synergy*.

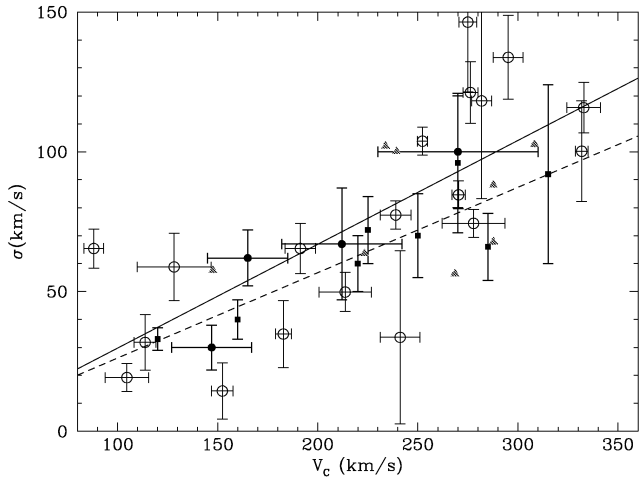

Figure 6. The radial stellar velocity dispersion at one scalelength for the inclined discs (filled squares) and the vertical one at $R = 0$ for the face-on discs (filled circles) of Bottema (1993). Open circles are the recent data of Vega Beltrán et al. (2001). The dashed and solid lines show, respectively, a simple fit to the data of Bottema (1993) and Vega Beltrán et al. (2001). The triangles correspond to galaxies of our sample for which a velocity dispersion is given in McElroy (1995).

to the prescriptions of the previous paragraph and Bottema's (1993) data, by combining equations (7) and (8). In the middle panel, we show the profile of the ratio of the gas surface density to the critical density, which is calculated either by equation (4) (i.e. by taking into account only the gas velocity dispersion, assumed here to be 6 km s^{-1} at all radii) or using equation (6) (i.e. by taking into account both the gaseous and the stellar components).

It can be seen that in the former case, the ratio $\Sigma_{\rm gas}/\Sigma_{\rm crit}$ remains roughly constant at an average value of ~ 0.65, between 4 and 14 kpc, i.e. in a large part of the star-forming disc; this value is very close to the value of 0.69 ± 0.20 that Martin & Kennicutt (2001) found as defining the SFR threshold in their sample of spiral galaxies (also shown as a grey-shaded area in Fig. 7). However, in the inner disc, i.e. in the 'molecular ring' where most of the star formation activity is concentrated, the values of $\Sigma_{\rm gas}/\Sigma_{\rm crit}$ are *below* the threshold found by Martin & Kennicutt (2001). The situation improves if the stellar radial dispersion profile is taken into account (solid curve in the middle panel of Fig. 7). Since, in the molecular ring one has $\Sigma_*\Sigma_{\rm gas} \sim 10$ and $\sigma_{\rm gas}\sigma_* \sim 0.1$, the resulting value of γ (equation 6) is $\sim \frac{1}{2}$ and $\Sigma_{\rm gas}/\Sigma_{\rm crit}$ increases in the inner Galaxy, up to the level of $\sim$1 in the molecular ring.

In the lower panel of Fig. 7 we present the SFR profile of the Milky Way (normalized to the solar neighbourhood SFR value), as given by various tracers (see Boissier & Prantzos 1999 for references to original data). It can be seen that the outer radius of the SFR profile of the Milky Way coincides with the radius of a steep decline in the $\Sigma_{\rm gas}/\Sigma_{\rm crit}$ profile; this conclusion is valid for both ways of calculating $\Sigma_{\rm crit}$.

To summarize, the Milky Way data

(i) support the idea of large-scale star formation according to the Toomre instability criterion of equation (2), since the value of $\Sigma_{\rm gas}/\Sigma_{\rm crit}$ is $\sim$constant across the star-forming disc,

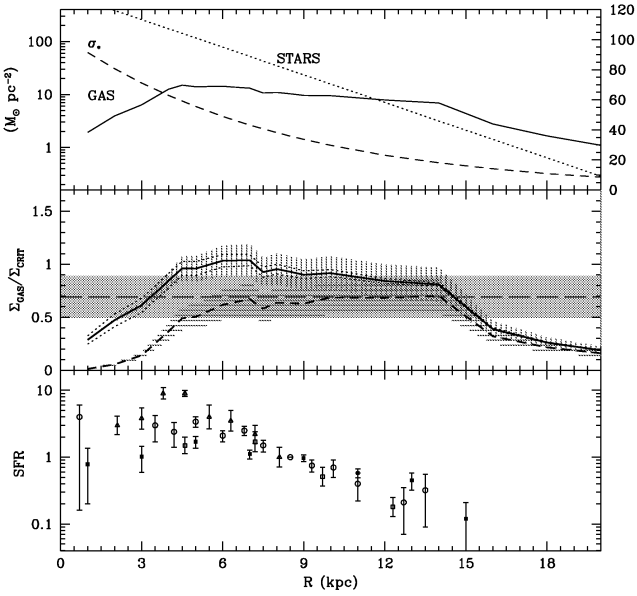

Figure 7. Gas, stars and star formation in the Milky Way disc. Upper panel, observed profiles of the total gas surface density (solid curve, H_2+H I, increased by 40 per cent to include He contribution, the H_2 being derived from CO with a metallicity-dependent conversion factor), the stellar profile (dotted curve exponential, with scalelength of 2.5 kpc and normalized to 42 $M_\odot$ pc^{-2} in the solar neighbourhood), and the stellar radial velocity dispersion (dashed curve, calculated according to equations 7 and 8, in km s^{-1} as indicated on the right axis). Middle panel, profile of the gas surface density to the critical density for two cases: first (dashed curve within horizontally hatched area, indicating the uncertainties on gas values), using equation (4) for Σ_{crit} (i.e. by taking into account only the gas velocity dispersion, assumed here to be 6 km s^{-1} at all radii); secondly (solid curve within vertically hatched area, indicating the uncertainties on gas values) using equation (6) for Σ_{crit} (i.e. including the contribution of the stellar disc to the instability criterion). The shaded area indicates the value 0.69 ± 0.20 that Martin & Kennicutt (2001) found for the star formation threshold in their sample of galactic discs. Bottom panel, SFR profile in the Milky Way (from various tracers), normalized to its value in the solar neighbourhood.

(ii) are consistent with the data of Martin & Kennicutt (2001) for a threshold of star formation in external spirals (at a value of $\Sigma_{gas}/\Sigma_{crit} \sim 0.7 \pm 0.2$ in most of the star-forming disc) and

(iii) favour the idea that the stellar component should also be used in the instability criterion (at least in the inner disc). This confirms the results of Wang & Silk (1994) who proposed this idea and tested it in the Milky Way.

Unfortunately, the situation with the other discs of our sample is not as clear-cut.

3.3 Thresholds for SF in galactic discs?

Fig. 8 shows the profiles of the ratio $\Sigma_{gas}/\Sigma_{crit}$ for the galaxies for which we have all the required information. The ratio was computed through equations (4) (circles) and (6) (squares). The epicyclic frequency was computed by adopting the analytical rotation curve of equation (2) (filled symbols), which was derived analytically. For seven galaxies, the high-resolution rotation curves of Sofue et al. (1999) were also used and derived numerically, with very similar results (see Fig. 8, open symbols); an exception was the case of NGC 5194, owing to its peculiar rotation curve. The absence of a difference between the two computations shows that the details of the rotation curve only affect the critical density slightly, compared with other quantities.

When the critical density is computed with only the gaseous component (equation 4), the discs are often found to be subcritical over large intervals of their radial extent. Eight of the galaxies of our sample (2903, 2403, 4258, 3031, 4571, 4501, 4654, 4651) are found to be subcritical with respect to the average threshold value of $\Sigma_{gas}/\Sigma_{crit} = 0.69 \pm 0.20$ found by Martin & Kennicutt (2001); the gas density is substantially lower than the critical value even in regions with intense observed star formation. The rest of our sample is equally divided between critical (2541, 5194, 4321, 4713) and overcritical galaxies (925, 4254, 4303, 4654); in the latter case the value of $\Sigma_{gas}/\Sigma_{crit}$ is considerably larger than the threshold value of Martin & Kennicutt (2001). We note that all three cases are encountered with similar frequencies in isolated and Virgo spirals, i.e. the environment does not seem to play a role in the overall disc instability.

As in the case of the Milky Way, including the stellar component in the instability criterion (equation 6) leads to larger values of the ratio $\Sigma_{gas}/\Sigma_{crit}$ in the whole disc. Only two discs still remain subcritical with the modified criterion (3031, 4571) and only marginally so. In a few cases (4303, 4654) the modified values of $\Sigma_{gas}/\Sigma_{crit}$ are three times larger than the threshold value found by Martin & Kennicutt (2001).

The average value of $\Sigma_{gas}/\Sigma_{crit}$ at the outer edge of the star-forming discs in our sample is 0.50 when only the gaseous component is included in the instability criterion and 0.73 when the stellar component is also included. As a result of the large variations between the values of $\Sigma_{gas}/\Sigma_{crit}$ in our discs, we find a large dispersion in the average threshold values: ± 0.33 in the former case and ± 0.38 in the latter, i.e. almost double the dispersion found by Martin & Kennicutt (2001).

We found that the evaluation of the H_2 profile in the outer parts of the galaxies is crucial for the derivation of $(\Sigma_{gas}/\Sigma_{crit})_{thres}$. When the H_2 surface density profile is not extrapolated beyond the last observed point (i.e. assuming that no molecular gas is present beyond that point), we obtain a threshold value $(\Sigma_{gas}/\Sigma_{crit})_{thres} = 0.32 \pm 0.16$. When a fit is performed to the H_2 profile, and extrapolated beyond the last observed point, the result is the previously mentioned value 0.50 ± 0.33; this is in agreement with the value of 0.69 ± 0.2 of Martin & Kennicutt (2001), who used the same assumption.

In conclusion, contrary to the case of the Milky Way disc, our analysis of external spirals does not find evidence supporting the application of the (original or modified) Toomre criterion for large-scale star formation; it is true, however, that the inclusion of the stellar component in the instability criterion makes most of our discs overcritical according to that criterion. Also, it is worth noting that stars are very often present beyond the threshold radius, as it can be seen on the photometric profiles (Fig. 2), suggesting that some star formation must have occurred in those regions in the past.

Our conclusions differ from those of Martin & Kennicutt (2001) despite the fact that we have a large number of galaxies in common (13 out of 16 in our sample). In their larger sample of 32 discs they find only seven subcritical ones (i.e. 22 per cent), whereas we find that eight of our 16 discs are subcritical. Among the galaxies in common, four were found to be subcritical in our study but not in Martin & Kennicutt (2001): NGC 2903, 4501, 4651, 4689. Inspection of Fig. 5 shows that the molecular gas represents a significant fraction of the total amount of gas over a large fraction of the disc within the threshold radius for these galaxies. At the same time, Fig. 1

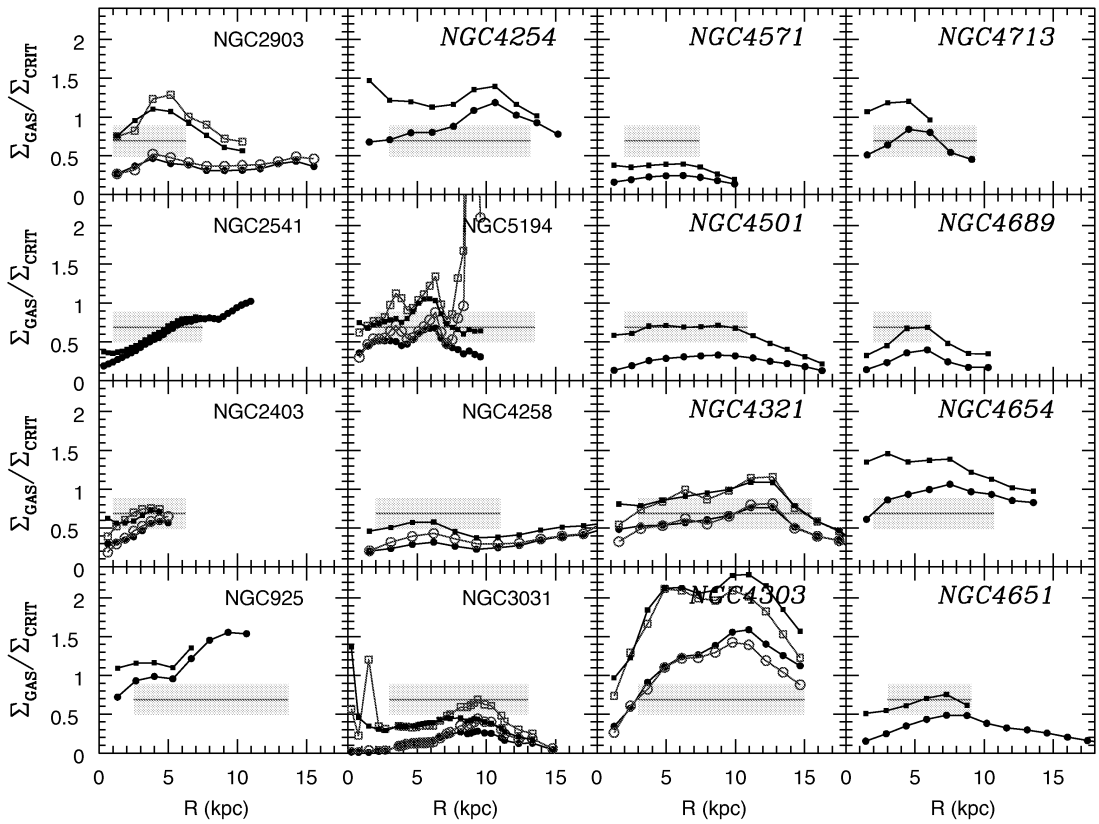

Figure 8. Ratio of the gas density to the critical density, when gas only is taken into account in the instability criterion (filled circles) and when the stellar density is taken into account (filled squares); the epicyclic frequency was computed using the analytical rotation curve of equation (2) (Section 2.7). When a high-resolution rotation curve was available (Sofue et al. 1999), the epicyclic frequency was derived numerically and the corresponding results are indicated by open circles and squares, respectively. The horizontal line and the shaded area at 0.69 ± 0.2 correspond to the threshold values for star formation found by Martin & Kennicutt (2001); the inner limit of that line corresponds to the bulge/disc limit and the outer one to the observed threshold in star formation (see Section 2.4). Galaxies with names in italics belong to the Virgo cluster. This figure is available in colour in the on-line version of the journal on *Synergy*.

indicates a quite large effect of the metallicity on the determination of the H_2 surface density: with a constant conversion factor, Martin & Kennicutt overestimate the amount of H_2 with respect to us. The differences in the fraction of subcritical discs and in the value of $(\Sigma_{gas}/\Sigma_{crit})_{thres}$ in our study and theirs mainly reflect differences in the evaluation of the conversion from CO to H_2.

We note that recently Wong & Blitz (2002) reached similar conclusions to us, concerning the validity of the Toomre criterion. Their analysis of a different sample of galaxies failed to show a clear relationship between the Q value and large-scale star formation. They note, however, that $Q \sim 1$ is often observed in galactic discs, while two discs with high Q values (subcritical) have small gas fractions; they suggest then that *Q is actually a measure of the gas fraction in the disc* and they support their suggestion with a rather qualitative analysis (see their Section 5.3).

We have used our detailed stellar and gas profiles to derive corresponding gas fraction profiles, computed as $\Sigma_{gas}/(\Sigma_{gas} + \Sigma_*)$, for all the galaxies of our sample and we plotted the Q values as a function of the gas fraction (Fig. 9). If Wong & Blitz (2002) were right, we would expect to find an anticorrelation between Q and the gas fraction, with large values of Q corresponding to low gas fractions. On the contrary, our results suggest no correlation between low values of the gas fraction and subcritical discs: nine of our discs are indeed subcritical at a gas fraction of $\sim$0.1, as argued by Wong and Blitz (2001), but seven are clearly critical. Also, we have several galaxies that are subcritical at gas fractions $\sim$1, whereas they should be critical according to Wong & Blitz (2002). Thus, our analysis does not support the idea that Q is a measure of the gas fraction in the disc.

4 THE STAR FORMATION LAW

4.1 Star formation versus gas amount

A comprehensive review of our current (lack of) understanding of large-scale star formation in galaxies has been presented recently by Elmegreen (2002), who also provides an extensive reference list on the subject.

Intuitively, star formation should be associated to the molecular content of a galaxy, rather than to the neutral gas amount. Such a correlation has indeed been claimed to be observed in spirals by Young and collaborators (e.g. Rownd & Young 1999), under the assumption of a constant conversion factor of CO to H_2. Similar conclusions were reached by Boselli et al. (1995), who showed that the molecular mass follows the star formation rate quite closely in luminous spirals; the galaxies of their sample display similar metallicities and the assumption of a constant conversion factor is then justified. However, it was argued by Boselli et al. (1995) that the scatter obtained for less luminous galaxies could be due to variations in the conversion factor. Boselli et al. (2002) showed recently that the conversion factor indeed depends on the physical properties of the

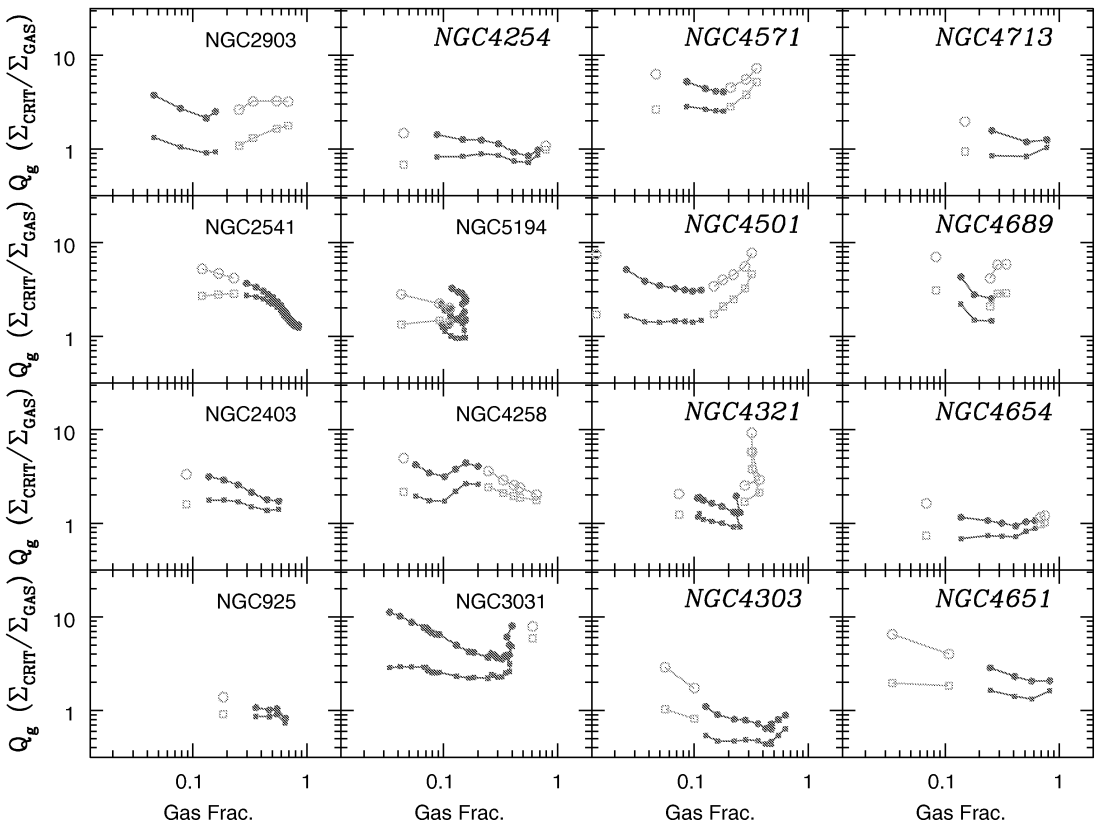

Figure 9. Ratio of the gas density to the critical density as a function of the gas fraction for all the discs of our sample, when gas only is taken into account in the instability criterion (circles) and when the stellar density is taken into account (squares). Filled symbols correspond to regions of active star formation (i.e. inside the shaded bars of Fig. 8) and open symbols to regions outside. This figure is available in colour in the on-line version of the journal on *Synergy*.

galaxy. Once a metallicity-dependent conversion factor is adopted, a good correlation is observed between H_2 and the star formation rate.

As discussed in Section 2.3, in this paper we adopted a metallicity-dependent conversion factor to compute the densities of H_2 within the discs of our sample. It can be seen in Fig. 10 that the resulting azimuthally averaged molecular gas surface density presents a better correlation with the star formation rate density than the neutral gas (left and middle panels, where the H_2 and SFR profiles have been smoothed to the H I resolution, and corrected for the He fraction by multiplying them by 1.4). The good agreement correlation between H_2 and the star formation rate in our analysis of azimuthally averaged quantities corroborates the findings of Boselli et al. (2002) concerning global quantities of the discs.

Instead of thinking of the star formation process as a sequence (neutral gas → molecular gas → stars), one may consider it as the result of dynamical processes involving the totality of the gas density. In that case, a better correlation should be found between the star formation rate and the total gas density rather than either the molecular or the neutral component. Indeed, since Schmidt (1959),

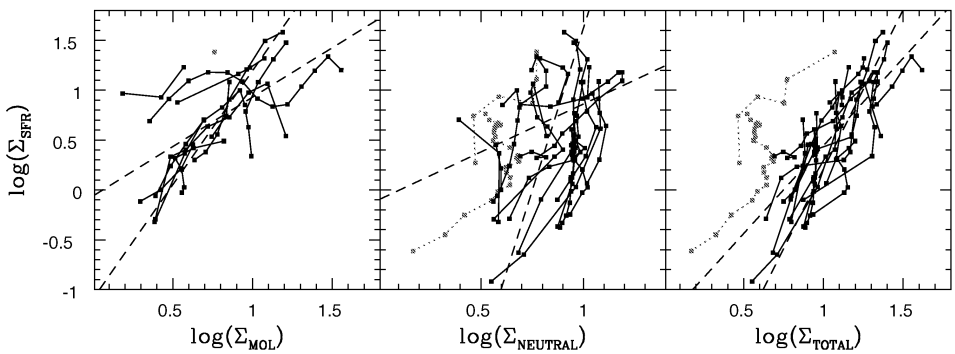

Figure 10. Star formation rate density as a function of molecular gas density (left), neutral gas density (middle) and total gas density (right); units are $M_\odot\ pc^{-2}\ Gyr^{-1}$ for the SFR and $M_\odot\ pc^{-2}$ for the gas (where the He fraction has been accounted for). The data are smoothed to the H I resolution. The solid curves connect points within the same galaxy. The dashed lines are the two regression fits in each case (see the text); the galaxies NGC 3031 and 4258 (indicated by the dotted curves are excluded from the fit.

there has been evidence that the star formation rate density ($\Sigma_{\rm SFR}$) is related to the total gas density ($\Sigma_{\rm gas}$) (Kennicutt 1998a):

$$\Sigma_{\rm SFR} = \alpha \Sigma_{\rm gas}^{n} \quad (1 < n < 2). \tag{9}$$

Basic models based on self-gravitating discs can produce such a 'Schmidt law' (e.g. Kennicutt 1998b). The right-hand panel of Fig. 10 displays a reasonably good correlation between the star formation rate and the gas density for most of the galaxies of our sample. Two galaxies that are rather peculiar can be easily identified on this plot. One of them is NGC 3031 which has a low gas content but a high star formation rate, especially in its inner part; this galaxy is forming stars despite being subcritical (Fig. 9). The other is NGC 4258 and displays a normal gas content but a larger efficiency to form stars compared with all the other galaxies in our sample.

We stress that the correlations displayed in Fig. 10 concern *azimuthally averaged* quantities, whereas Boselli et al. (2002) or Kennicutt (1998a) studied such correlations between global quantities or averaged over the whole disc (inside the optical radius).

The Schmidt law is the most widely used, but other semi-empirical 'recipes' of star formation have been suggested for galactic discs (and implemented in relevant models).

Ohnisi (1975) suggested that star formation is enhanced by the passage of spiral density waves with a frequency $\Omega(R) - \Omega_{\rm P}$, where $\Omega(R)$ is the rotational frequency of the galaxy at radius R and $\Omega_{\rm P}$ the frequency of the spiral pattern; for $\Omega(R) \gg \Omega_{\rm P}$ this leads to a star formation rate SFR $\propto \Omega(R) \propto V(R)/R$, where $V(R)$ is the corresponding rotational velocity (see also Wyse & Silk 1989). According to Larson (1988) the presence of the $\Omega(R)$ factor in the radial variation of the star formation rate could also be obtained if a self-regulation of star formation occurs such that $\Sigma_{\rm gas} \sim \Sigma_{\rm crit}$. Kennicutt (1998a) has indeed found that the observed averaged (over the optical radius) densities of the star formation rate and the total gas density are related equally well either by a simple Schmidt law (equation 9) or by the form

$$\Sigma_{\rm SFR} = \alpha \Sigma_{\rm gas} / \tau_{\rm dyn}, \tag{10}$$

where $\tau_{\rm dyn} \sim R/V(R)$ is the dynamical time-scale at radius $R = R_{\rm opt}$.

In Boissier & Prantzos (1999), a 'semitheoretical' SFR deduced from those consideration was adopted:

$$\Sigma_{\rm SFR} = \alpha \Sigma_{\rm gas}^{n} V/R \tag{11}$$

(with V being the rotational velocity, taken as constant and equal to 220 km s^{-1} for the Milky Way). The index n was chosen to be $n = 1.5$ on an empirical basis [providing the observed relation between $\Sigma_{\rm SFR}(R)$ and $\Sigma_{\rm gas}(R)$ and reproducing the observed abundance gradient]. This theoretical star formation rate was adopted in subsequent models extended to all spiral galaxies, which successfully reproduced their global properties (Boissier & Prantzos 2000; Boissier et al. 2001) and their abundance and colour gradients (Prantzos & Boissier 2000).

Another star formation law, sometimes used in models of chemical evolution (e.g. Matteucci & Chiappini 2001) was suggested by Dopita & Ryder (1994) on the basis of an observed correlation between the stellar surface density (as traced by I-band photometry) and the star formation rate:

$$\Sigma_{\rm SFR} = \alpha \Sigma_{\rm gas}^{n} \Sigma_{\rm T}^{m}, \tag{12}$$

where $\Sigma_{\rm T}$ is the total surface density (gas plus stars). Dopita & Ryder (1994) tested this law only indirectly (via a model, since they had no gas data available) and found it to be consistent with observations if $n + m$ is between 1.5 and 2.5. They also presented a model of stochastic self-regulating star formation, predicting $n = \frac{5}{3}$ and $m = \frac{1}{3}$, values that are in agreement with their empirical findings.

4.2 Empirical determination of SF parameters

We tested the three SF laws of equations (9), (11) and (12) with our data (with all the data being smoothed to the H I resolution). The gas profile was multiplied by a factor of 1.4 to take into account the He contribution. The H_2 data were extrapolated assuming an exponential profile (see below for a discussion of this assumption). Equation (11) requires the rotational velocity $V(R)$, that we simply approximated by the analytical rotation curve of equation (2). For equation (12) we need an estimate of the total surface density, that is of the stellar density; the photometric H-band profiles, barely affected by dust extinction, were used for that purpose, assuming the same mass-to-luminosity ratio ($M_*/L_{\rm H}$) as in Boissier et al. (2001).

Fig. 11 shows our data plotted in the plane $\Sigma_{\rm gas}$ versus $\Sigma_{\rm SFR}$ (top, testing equation 9), in the plane $\Sigma_{\rm gas}$ versus $\Sigma_{\rm SFR} \times R/V(R)$ (middle,

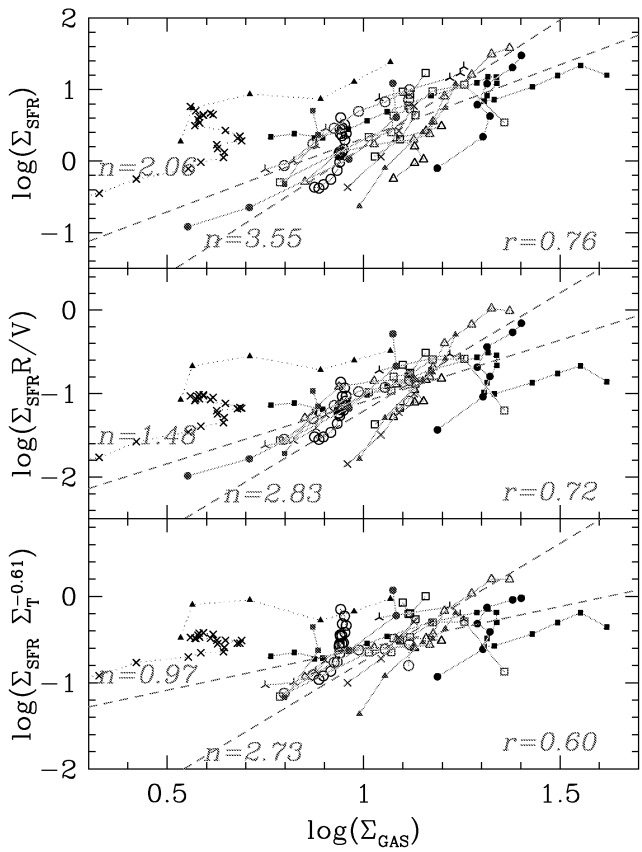

Figure 11. Test of various star formation laws. Top, gas surface density versus star formation rate surface density (testing the standard Schmidt law, equation 9). Middle, gas density versus $\Sigma_{\rm SFR} \times R/V(R)$ (testing equation 11). Bottom, gas density versus $\Sigma_{\rm gas}^{n} \Sigma_{\rm T}^{-0.61}$ (testing a Dopita–Ryder law, equation 12, with the best value of the second parameter $m = 0.61$). The grey lines connect points of the same galaxy (the dotted lines correspond to NGC 4258 and 3031, not considered in the fits, see Section 4.2). Different symbols are used for different galaxies. The dashed lines show two fits, one minimizing deviations on $\Sigma_{\rm SFR}$ (the one that should be used for a determination of the SFR parameters) and one minimizing deviations on $\Sigma_{\rm gas}$. The corresponding index n is indicated for each one of them and is also reported on Table 3. The correlation coefficient (r) is indicated in the bottom right-hand part of each panel. This figure is available in colour in the on-line version of the journal on *Synergy*.

testing equation 11) and in the plane $\Sigma_{\rm gas}$ versus $\Sigma_{\rm SFR} \times \Sigma_{\rm gas}^{n} \Sigma_{\rm T}^{-0.61}$ (bottom, testing equation 12). In the last case, the best-fitting value for the second parameter m was adopted for the figure (i.e. the one minimizing χ^2 for the SFR).

The points corresponding to a single galaxy are connected by a grey line. The dashed lines show simple least-squares fits, one minimizing the deviation on the SFR density, and one on the gas surface density (the difference between the indices in each case gives an idea of the dispersion of the relation). Since we are searching for the 'best-fitting law' of the SFR, we will adopt for the discussion the first of these two fits.

The dotted lines correspond to NGC 3031 and 4258. The latter is obviously an outlier, having quite low gas density but relatively high SFR (see Fig. 5) and we do not consider it in the fits; note that high-resolution CO data for this galaxy differs from the low-resolution ones (see Section 2.3). We also ignored NGC 3031, because its gaseous profile (H I and total) is very atypical (see Fig. 5). It is the only object in our sample with a low gas density over the whole disc. NGC 3031 is indeed among the more subcritical discs of Martin & Kennicutt (2001).

One would expect that the outlying or peculiar galaxies in Fig. 11 (and in Figs 8–10) could be systematically associated to the cluster environment, H I deficient objects, or have a peculiar morphology. We do not find obvious trends in our small sample, however, the analysis of Gavazzi et al. (2002) on integrated quantities has shown that cluster H I deficient galaxies have, on average, lower star formation activities than their field counterparts.

For a simple Schmidt law (equation 9), the least-squares fit gives an index $n \sim 2$, steeper than the 1.4 suggested by Kennicutt (1998b) or the 1.3 ± 0.3 of his earlier work (Kennicutt 1989). When a dynamical factor is introduced (equation 11), we obtain $n \sim 1.5$, steeper again than the slope $n \sim 1$ found by Kennicutt (1998b). However, the introduction of Ω in both studies acts in the same direction: it reduces the value of n.

The differences between our results and those of Kennicutt (1998b) may be due to several reasons. (i) Kennicutt (1998b) uses surface densities averaged within the optical radius, i.e. he includes the bulge region (while we only study the star-forming disc) and in some cases he also includes some gas located beyond the threshold radius (while we work on radial profiles within the radial range of interest). (ii) The law obtained by Kennicutt (1998b) was established on a large range of gas surface density (an astonishing factor of 10^5) by introducing in the sample starburst galaxies; however, for normal discs only, his analysis also showed a large dispersion of the index n, with values ranging from 1.29 for a standard least-squares fit to 2.47 for a bivariate least-squares regression (for a standard Schmidt law, equation 9). The corresponding values in our case are, respectively, 2. and 2.6. (iii) We use a conversion factor between CO and H_2 that depends explicitly on the metallicity, while he adopts a constant conversion factor. This important point also applies to the comparison of our work and that of Kennicutt (1989), also based on radial profiles of spiral galaxies. (iv) The galaxy sample is different; it is obvious from Fig. 11 that star formation in galaxies does not obey a well-defined relation but presents a large scatter around an average. The SFR law can then be defined only in a statistical sense, and since the number of galaxies for which such studies can be performed is still small, it is understandable that studies with different samples produce different results.

Wong & Blitz (2002) used a small sample of seven galaxies only, but with higher spatial resolution. Assuming a uniform model of extinction (comparable to the present work) they found for the simple Schmidt law a value of $n = 1.1$, i.e. they found a relation less steep than both us and Kennicutt (1998b). On the other hand, assuming a dependence of extinction on the gas column density they found $n = 1.7$. They also found that an SFR of the form $\Sigma_{\rm gas}\Omega$ is compatible with their data, but only if an important radially dependent extinction is assumed. However, they did not attempt to fit a law of the form of equation (11).

The differences between our work and Wong & Blitz (2002) may result from: (i) the small statistics (as previously discussed); (ii) the fact that the galaxies of Wong & Blitz (2002) are selected to be bright in CO, i.e. H_2-rich, which may introduce some bias in the sample, as these authors also acknowledge; (iii) the sensitivity of the obtained index n to the assumed extinction gradient, which is difficult to evaluate since it also depends on the abundance gradient, and since the observed scatter at a given radius is stronger than that gradient (Martin & Kennicutt 2001). (iv) The assumption of a constant conversion factor of CO to H_2.

Finally, we tested the SF law proposed by Dopita & Ryder (equation 12) with the subsample for which the stellar density profile is available from H-band photometry. A simple least-squares fit (minimizing the deviation on $\Sigma_{\rm SFR}$) to our data leads to $n \sim 1$ and $m \sim 0.61$, substantially different from the values of $\frac{5}{3}$ and $\frac{1}{3}$ obtained by Dopita & Ryder (1994).

The results presented in Fig. 11 are obtained by adopting the analytical rotation curve of equation (2) and an extrapolation of the molecular gas profile, as described in Section 3. To test the effect of these assumptions, we performed the same work assuming that there is no molecular gas beyond the last CO detection point. The difference in the slopes of the relationships are presented in Table 3.

Table 3. Slopes of the star formation laws under two different assumptions on the molecular content at large radii. The values of the exponent n are given for the two regression lines in each case. For the Dopita–Ryder law, the 'best-fitting' value of the second parameter (m) was assumed. Note that adopting a flat rotation curve barely affects the values of n for the $\Sigma_{\rm gas}^{n}\Omega$ law.

$\Sigma_{\rm SFR}$	No H_2 extrapolation	H_2 extrapolation
$\propto \Sigma_{\rm gas}^{n}$	1.96 (3.1)	2.06 (3.55)
$\propto \Sigma_{\rm gas}^{n}\Omega$	1.38 (2.52)	1.48 (2.83)
$\propto \Sigma_{\rm gas}^{n}\Sigma_{\rm T}^{m}$	1.00 (2.21) for $m = 0.56$	0.97 (2.73) for $m = 0.61$

The differences are relatively modest, contrary to what occurred for the threshold, since the fits are essentially determined by the data concerning the main body of the molecular disc.

Adopting a flat rotation curve instead of the analytical rotation curve of equation (2) also leads to small differences: we obtain a slightly lower slope (1.28 in the case of no H_2 extrapolation and 1.32 in the case of H_2 extrapolation) for a flat rotation curve compared with the analytical rotation curve (1.38 and 1.48, respectively).

In conclusion, the SF laws that we obtained depend only weakly on assumptions concerning the rotation curve and the molecular gas profile in the outer disc.

4.3 Application to the Milky Way

In the previous section, we determined the parameters of three widely used star formation laws (equations 9, 11, 12) by means

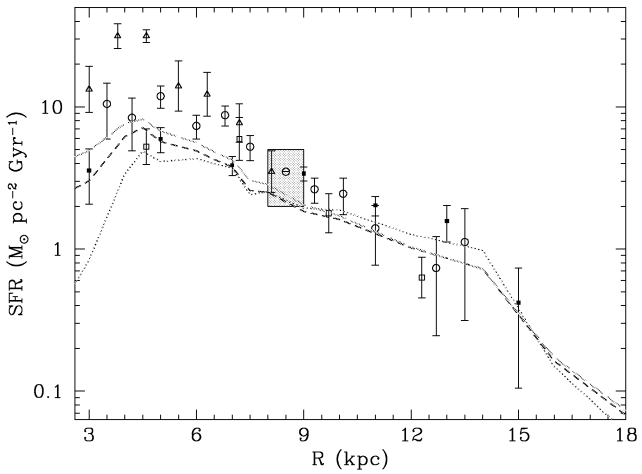

Figure 12. Application of the three SF laws obtained in Section 4.2 (pure Schmidt, dotted; Schmidt modified by rotation, short-dashed; and Schmidt modified by stellar density, long dashed). They are compared with various SF tracers in the disc of the Galaxy (see Section 4.3 for references). This figure is available in colour in the on-line version of the journal on *Synergy*.

of our galaxy sample. As in the case of the SF threshold (see Section 3.2), it is interesting to see how the resulting SF laws match the star formation data of the Milky Way disc.

Using the well-known gaseous and stellar radial profiles of the Milky Way and a flat rotation curve [$V(R) = 220$ km s^{-1}], we calculated the corresponding SF profiles; the results are displayed in Fig. 12, respectively, for the simple Schmidt law (dotted curve), the Schmidt law modified by the dynamical factor V/R (short-dashed curve) and the Schmidt law modified by the stellar density (long-dashed curve). We compare the results to the SF radial profile of the Galaxy, as estimated through various tracers (Guibert, Lequeux & Viallefond 1978; Gusten & Mezger 1983; Lyne, Manchester & Taylor 1985; Case & Bhattacharya 1998). Note that the observations were scaled to the value of the SFR in the solar neighbourhood, which has its own uncertainty; the box in the centre of the figure indicates the range of its possible values (Rana 1991).

The three SF laws produce quite similar results in the range 4–18 kpc, i.e. over the whole radial extent of the disc. The pure Schmidt law fails considerably in the inner disc (inside 3 kpc), since the low amounts of gas there do not allow it to reproduce the relatively high values of observed SFR. All three laws give satisfactory results in the 4–15 kpc range, while the modified Schmidt laws also fit the observations in the inner disc; however, due to several complications that might arise in that region (i.e. the role of the bar in star formation) the 'success' of the modified Schmidt laws in that region should not be considered as a 'proof' a their validity.

In summary, data for the Milky Way disc are compatible with all three SF laws that we empirically determined in the previous section. Only a consistent application of those SF laws in a chemical evolution model of the Milky Way could (perhaps) favour one of these SF laws over the others, by comparison with as many observed radial profiles as possible (e.g. chemical and photometric profiles, as in the work of Boissier & Prantzos 1999 for the gaseous, chemical and photometric profiles of the MW disc). We note, however, that in practice, even this test may not be conclusive, because of the poorly known radial and temporal dependence of the gas infall rate on the disc. Gaseous infall is indeed required, at least in the solar neighbourhood to account for the so-called 'G-dwarf problem' (e.g. Pagel 1997 and references therein).

5 SUMMARY

In this paper we present a detailed study of the properties of star formation in disc galaxies. We use an extended data set, consisting of (azimuthally averaged) radial profiles of stellar and gaseous (atomic and molecular) surface densities, of star formation rates and rotation curves. The molecular gas is derived from CO with a metallicity-dependent conversion factor for the first time in this kind of study. These data allow questions related to the star formation rate and to the existence of a star formation threshold in galactic discs to be studied. Our sample comprises 16 disc galaxies, approximately half of which belong to the Virgo cluster.

Our results may be summarized as follows. The existence of a star formation threshold in our discs was studied using the Toomre (1964) instability criterion and using either the gaseous component alone or both the gaseous and stellar components in the definition of the instability parameter Q. In the latter case, the profile of stellar velocity dispersion is also required and we calculated it for our discs based on the observations of Bottema (1993). We also used both analytical and observed rotation curves for the evaluation of Q.

We find that only half of our sample galaxies are overcritical (i.e. locally unstable and prone to form stars) when the gaseous component alone is taken into account, even in disc regions where observations indicate that vigorous star formation is taking place. Including the stellar component improves the situation substantially, since only two discs remain subcritical then (and only marginally so).

These results refer to an average value of the instability parameter $Q = 0.70 \pm 0.20$ (i.e. slightly lower than unity), as determined observationally by Martin & Kennicutt (2001) with a larger disc sample (32 galaxies). Our own Q value, determined at the termination of the SF profile, is similar to the above value when the stellar component is included and slightly lower when it is ignored (0.71 and 0.5, respectively). However, in both cases, corresponding uncertainties are larger than found by Martin & Kennicutt (0.38 and 0.33, respectively, compared with 0.20 in their case).

We find that the instability criteria apply fairly well to the Milky Way disc, where Q values are systematically $\sim$0.7 when the gaseous component alone is used and $\sim$0.9–1 when the stellar component is also included. We find it encouraging that the galaxy with the best defined profiles shows such an exemplary behaviour. We think that the large dispersion in the Q values found in our sample result (at least partly) from systematic uncertainties in the various profiles entering the evaluation of Q. Among them, of crucial importance are: (i) the conversion factor of CO emission to the H_2 gas amount (we use a metallicity-dependent conversion factor, unlike previous studies) and, even more so (ii) the extrapolation of the H_2 profile beyond the last observed point. These factors explain to a large extent the quantitative differences between our results and those of Martin & Kennicutt (2001) and Wong & Blitz (2002). In particular, our findings do not support the claim of Wong & Blitz (2002) that Q is actually a measure of the gas fraction in the discs.

In agreement with Wong & Blitz (2002) we find that the observed local (i.e. at a given radius) SF rate density correlates better with the total gas density or with the molecular gas density than with the neutral gas density. We analysed three local SF laws with our data: a pure Schmidt law SFR $\propto \Sigma_{\rm gas}^n$, a Schmidt law modified by the disc rotational frequency SFR $\propto \Sigma_{\rm gas}^n V(R)/R$, and a Schmidt law modified by the local surface density $\Sigma_{\rm T}$: SFR $\propto \Sigma_{\rm gas}^n \Sigma_{\rm T}^m$ (according to a suggestion by Dopita & Ryder 1994).

We find that the modified Schmidt laws do slightly better than the pure Schmidt law, as expected in view of their supplementary degrees of freedom. We also find a larger index n for the gaseous component than Kennicutt (1998b), both for the pure Schmidt law and for the one modified by rotation (2 and 1.5, compared with 1.4 and 1, respectively). We note that Kennicutt's analysis included starbursts, so that his gas surface densities covered five decades in magnitude, instead of $\sim$1.5 decade in our case; by limiting his analysis to the low surface density normal spirals, Kennicutt (1998) also found larger values of n, close to ours. Besides, his analysis concerned only averaged quantities over the galactic discs, whereas ours concerns azimuthally averaged quantities, a fact that certainly explains the largest dispersion and the poorest fits that we obtain. On the other hand, Wong & Blitz (2002) used only azimuthally averaged quantities in their study and found values of $n = 1.1$ for a uniform extinction model and 1.7 for an extinction dependent on the column density in the case of the pure Schmidt law; the latter case corresponds more closely to our own results.

Again, we find that the three derived SF laws apply fairly well to the data of the Milky Way disc, although the pure Schmidt law fails in the inner Galaxy (where the situation is uncertain anyway, due to the poorly known role of the galactic bar). The exemplary behaviour of the Milky Way disc makes us think that (either it is exceptional or) a much more systematic work than this one could allow one to determine much better the local properties of star formation in discs. Such a work should involve: a much larger number of (unperturbed) discs than used here; much more extended and detailed radial profiles, especially in the case of molecular gas (for instance, the results of the recent BIMA survey, Regan et al. 2001); and, above all, a much better understanding of the various systematic uncertainties of the problem, for instance concerning the absolute local values of the star formation rate and the role of non-axisymmetric profiles.

REFERENCES

Adler D.S., Westpfahl D.J., 1996, AJ, 111, 735
Begeman K.G., 1987, PhD thesis, Kapteyn Institute
Boissier S., Prantzos N., 1999, MNRAS, 307, 857
Boissier S., Prantzos N., 2000, MNRAS, 312, 398
Boissier S., Boselli A., Prantzos N., Gavazzi G., 2001, MNRAS, 321, 733
Boselli A., Gavazzi G., 2002, A&A, 386, 124
Boselli A., Gavazzi G., Lequeux J., Buat V., Casoli F., Dickey J., Donas J., 1995, A&A, 300, L13
Boselli A., Tuffs R.J., Gavazzi G., Hippelein H., Pierini D., 1997, A&AS, 121, 507
Boselli A., Gavazzi G., Franzetti P., Pierini D., Scodeggio M., 2000, A&AS, 142, 73
Boselli A., Gavazzi G., Donas J., Scodeggio M., 2001, AJ, 121, 753
Boselli A., Lequeux J., Gavazzi G., 2002, A&A, 384, 33
Boselli A., Gavazzi G., Sanvito G., 2003, A&A, 402, 37
Bottema R., 1993, A&A, 275, 16
Boulanger F., Viallefond F., 1992, A&A, 266, 37
Braine J., Combes F., Casoli F., Dupraz C., Gerin M., Klein U., Wielebinski R., Brouillet N., 1993, A&AS, 97, 887
Broeils A., van Woerden H., 1994, A&AS, 107
Case G., Bhattacharya D., 1998, ApJ, 504, 761
Chincarini G., de Souza R., 1985, A&A, 153, 218
Dickey J.M., Hanson M.M., Helou G., 1990, ApJ, 352, 522
Distefano A., Rampazzo R., Chincarini G., de Souza R., 1990, A&AS, 86, 7
Dopita M., Ryder S., 1994, ApJ, 430, 163
Drozdovsky I.O., Karachentsev I.D., 2000, A&AS, 142, 425
Elmegreen B.G., 1987, Proc. IAU Symp. 115, Star Forming Regions. Kluwer, Dordrecht, p. 457
Elmegreen B.G., 2002, ApJ, 577, 206
Feldmeier J.J., Ciardullo R., Jacoby G.H., 1997, ApJ, 479, 231
Freedman W. et al., 2001, ApJ, 553, 47
Garnett D., Shields G., Skillman E., Sagan S., Dufour R., 1997, ApJ, 489, 63
Gavazzi G., 1987, ApJ, 320, 96
Gavazzi G., Boselli A., Pedotti P., Gallazzi A., Carrasco L., 2002, A&A, 396, 449
Gavazzi G., Boselli A., Donati A., Franzetti P., Scodeggio M., 2003, A&A, 400, 451
Guhathakurta P., van Gorkom J.H., Kotanyi C.G., Balkowski C., 1988, AJ, 96, 851
Guibert J., Lequeux J., Viallefond F., 1978, A&A, 68, 1
Gusten R., Mezger M., 1983, Vistas Astron., 26, 159
Haynes M., Giovanelli R., 1984, AJ, 89, 758
Huchtmeier W.K., Richter O.-G., 1989, A General Catalog of H I Observations of Galaxies, The Reference Catalog, XIX, 350. Springer-Verlag, Berlin, p. 8
Jarrett T.H., Chester T., Cutri R., Schneider S., Huchra J., 2002, AJ, 125, 525
Kennicutt R.C., 1989, ApJ, 344, 685
Kennicutt R.C., 1998a, ARA&A, 36, 189
Kennicutt R.C., 1998b, ApJ, 498, 541
Larson R.B., 1988, in NATO ASIC Proc. 232, Galactic and Extragalactic Star Formation, p. 459
Lyne A., Manchester R., Taylor J., 1985, MNRAS, 213, 613
McElroy D.B., 1995, ApJS, 100, 105
Martin C., Kennicutt R., 2001, ApJ, 555, 301
Matteucci F., Chiappini C., 2001, New Astron. Rev., 45, 567
Nakai N., Kuno N., 1995, PASJ, 47, 761
Nilson P., 1973, Uppsala general catalogue of galaxies, Acta Universitatis Upsaliensis. Nova Acta Regiae Societatis Scientiarum Upsaliensis – Uppsala Astronomiska Observatoriums Annaler. Astronomiska Observatorium, Uppsala
Ohnisi T., 1975, Progr. Theor. Phys., 53, 1042
Pagel B., 1997, Nucleosynthesis and Galactic Chemical Evolution. Cambridge Univ. Press, Cambridge
Pierini D., Gavazzi G., Boselli A., Tuffs R., 1997, A&AS, 125, 293
Pisano D.J., Wilcots E.M., Elmegreen B.G., 1998, AJ, 115, 975
Prantzos N., Boissier S., 2000, MNRAS, 313, 338
Quirk W.J., 1972, ApJ, 176, L9
Rana N., 1991, ARA&A, 29, 129
Rand R., Kulkarni S., Rice W., 1992, ApJ, 390, 66
Regan M.W., Thornley M.D., Helfer T.T., Sheth K., Wong T., Vogel S.N., Blitz L., Bock D.C.-J., 2001, ApJ, 561, 218
Romeo A.B., 1992, MNRAS, 256, 307
Rots A., 1975, A&A, 45, 43
Rownd B.K., Young J.S., 1999, AJ, 118, 670
Rubin V.C., Waterman A.H., Kenney J.D.P., 1999, AJ, 118, 236
Sage L., 1993, A&A, 272, 123
Sanders D.B., Solomon P.M., Scoville N.Z., 1984, ApJ, 276, 182
Schaye J., 2002, ApJ, submitted (astro-ph/0205125)
Schmidt M., 1959, ApJ, 129, 243
Silk J., 1997, ApJ, 481, 703
Skillman E.D., Kennicutt R.C., Shields G.A., Zaritsky D., 1996, ApJ, 462, 147
Sofue Y., Tutui Y., Honma M., Tomita A., Takamiya T., Koda J., Takeda Y., 1999, ApJ, 523, 136
Sperandio M., Chincarini G., Rampazzo R., de Souza R., 1995, A&AS, 110, 279
Toomre A., 1964, ApJ, 139, 1217
Toomre A., 1981, The structure and evolution of normal galaxies. Cambridge Univ. Press, Cambridge, p. 111
van der Kruit P.C., 1974, ApJ, 192, 1
van Zee L., Salzer J., Haynes M., O'Donoghue A., Balonek T., 1998, AJ, 116, 2805

Vega Beltrán J.C., Pizzella A., Corsini E.M., Funes J.G., Zeilinger W.W., Beckman J.E., Bertola F., 2001, A&A, 374, 394
Wang B., Silk J., 1994, ApJ, 427, 759
Warmels R., 1986, PhD thesis, Groningen Rijksuniversiteit
Wevers B., van der Kruit P., Allen R., 1986, A&AS, 66, 505
Wong T., Blitz L., 2002, ApJ, 569, 157
Wyse R.F.G., Silk J., 1989, ApJ, 339, 700
Young J.S. et al., 1995, ApJS, 98, 219
Zaritsky D., Kennicutt R., Huchra J., 1994, ApJ, 420, 87

This paper has been typeset from a TEX/LATEX file prepared by the author.